

Biomechanical changes on the typical sites of pressure ulcers in the process of turning over from supine position: theoretical analysis, simulation and experiment

Peng Su (✉ supeng@bistu.edu.cn)

Beijing Information Science and Technology University - Qinghe Xiaoying Campus: Beijing Information Science and Technology University

Qinglong Lun

Beijing Information Science and Technology University

Da Lu

BeiHang University School of Biological Science and Medical Engineering

Qiulong Wu

Beijing Information Science and Technology University

Tian Liu

Beijing Information Science and Technology University

Leiyu Zhang

Beijing University of Technology

Research Article

Keywords: turning over, pressure ulcers, contact pressure, biomechanical simulation, rehabilitation technical aids

Posted Date: August 2nd, 2021

DOI: <https://doi.org/10.21203/rs.3.rs-772442/v1>

License:  This work is licensed under a Creative Commons Attribution 4.0 International License.

[Read Full License](#)

Version of Record: A version of this preprint was published at Annals of Biomedical Engineering on April 8th, 2022. See the published version at <https://doi.org/10.1007/s10439-022-02938-9>.

1 **Biomechanical changes on the typical sites of pressure ulcers**
2 **in the process of turning over from supine position:**
3 **theoretical analysis, simulation and experiment**

4 Peng Su¹, Qinglong Lun¹, Da Lu², Qiulong Wu¹, Tian Liu¹,
5 Leiyu Zhang^{3*},

6 **ABSTRACT**

7 Background: Pressure ulcer is a typical disease, which is common in long-term
8 bedridden patients and difficult to cure. It is necessary to study the biomechanics of
9 the typical sites of pressure ulcers in turning over from supine position, which is an
10 important reference for clinical medical nursing and guides an assisted
11 exoskeleton robot design.

12 Methods: The typical sites of pressure ulcers mainly focus on the scapula and the
13 hip-sacrum of the trunk in turning over from the supine position. Based on the
14 requirements of rehabilitation technical aids and the anatomy theory, the simple
15 model of the scapula and the hip-sacrum were established for a force analysis in the
16 process of turning over from the supine position, and the theoretical contact pressure
17 between the human body and the bed surface was obtained. Then, three-dimensional
18 models of the scapula and hip- sacrum were reconstructed and the maximum stress
19 under different boundary conditions was obtained by finite element analysis. Finally,
20 the pressure distribution sensor was used to carry out the human experiment of
21 turning over from the supine position, and the pressure cloud diagram and the
22 maximum contact pressure curve of the shoulder blade and the hip were obtained

* Correspondence information: zhangleiyu1988@126.com; ³Beijing Key Laboratory of Advanced Manufacturing Technology, Beijing University of Technology, No.100 Pingleyuan, Chaoyang District, Beijing100124, China. Full list of author information is available at the end of the article.

23 under different angles of turning over.

24 **Results:** The results from theoretical analysis, simulation and experiment were
25 almost the same change trends, and the curves and the stress diagrams showed the
26 contact pressure change of the typical sites of pressure ulcers in turning over. The
27 angle threshold of the optimal comprehensive pressure can improve the use
28 efficiency of the equipment to assist human turning over and reduce the incidence of
29 pressure ulcers in the use of assisted bed in long-term bedridden patients.

30 **Conclusions:** In response to the less research on the mechanism of pressure ulcer,
31 biomechanical changes have been revealed, which helps to explain the causes of
32 pressure ulcer disease and provide basis for improving clinical nursing, and the
33 relevant results provided a reference that contributes to the man-machine coupling
34 design of the assisted rollover robot.

35 **Key word:** turning over, pressure ulcers, contact pressure, biomechanical
36 simulation, rehabilitation technical aids

37 **Background**

38 The pressure ulcer, also known as decubitus, is localized injury to the skin and/or
39 subcutaneous tissue caused by pressure or pressure in combination with shearing
40 force [1]. This phenomenon has a physiological effect restricting blood flow, with
41 the restriction in blood flow, perfusion of oxygen is limited and removal of
42 metabolic waste is inhibited which leads to cells death in the affected area resulting
43 in ischemia followed by pressure ulcers formation [2]. Pressure ulcers usually occur
44 in areas of bony prominence, for instance, the elbow, heel and back of skull, and
45 Multiple mechanical parameters including friction, shear stress, pressure and
46 microclimate are believed to be included in the potential triggering factors [3-6]. It is
47 more cost-effective to prevent the occurrence of ulcers than provide treatment

48 especially for the stage four ulcers [7]. The risk of death after suffering the pressure
49 ulcers will increase 4-fold in the critical patients [8]. Nevertheless, the incidence of
50 pressure ulcers can decrease by 50-60% through effective prevention [9]. So it is
51 significant to study the biomechanics of the typical sites of pressure ulcers in turning
52 over from supine position, and it helps to achieve better care.

53 The prevention of pressure ulcers is mainly about relieving backpressure, decrease
54 the exposure time and improving skin health [10]. The common method is to change
55 the patient's body position every two hours by turning over, and as technology
56 advances, rehabilitation robots may also be used that needs to have good
57 human-machine coupling [11-13]. Seo et al. discussed the development of an
58 intelligent bed robot system, and monitoring using an array of pressure sensors, the
59 bed posture and movement of the patients were measured and evaluated [14]. Some
60 scholars model the bones and muscles of the human body movement system based
61 on the skeletal structure, and other studies on how to prevent pressure ulcers are
62 in-depth discussion [15]. Recently the new type sheet with low friction and
63 optimized moisture transfer properties has been studied, which may be used to
64 prevent pressure ulcers because of its lower friction properties compared with a
65 common medical sheet [16-18]. Furthermore, the relationship between the contact
66 pressure and the supine angle was studied by researchers. They conclude that the
67 minimum and maximal contact pressures of the sacrum are in a supine angle of 30°
68 and 90° [19].

69 Current research on pressure ulcer care mainly focuses on the pressure relief
70 equipment such as the decompression mattress or rehabilitation robot. There are few
71 investigations into the biomechanics of human structure leading to pressure ulcers.
72 According to the structure of the body, the scapula, sacrum and calcaneus form a

73 plane and support the entire body weight in the supine position [20], and the tilting
74 can affect the strain distribution, taking away the highest peak strains of the sacrum.
75 In different parts of the body, the probability of pressure ulcers is different, and in the
76 same area, there are biomechanical changes in the process of turning over. It is
77 necessary to reveal the biomechanics mechanism leading to pressure ulcers in order to
78 better guide pressure ulcers care, such as the optimal care angle and the specific care
79 position.

80 For the purpose of explaining the biomechanical mechanism of human turning
81 over movement from supine position, the paper explores the interaction between the
82 typical sites of pressure ulcers and stress condition in the process of turning over
83 from supine position, then the result of the experiment in which the body side turn
84 90° can be observed. After that, this paper implements three-dimensional
85 reconstruction of the human skeleton with the help of CT (Computed tomography)
86 scan image and finite element analysis by ABAQUS to analyze the stressful
87 condition of human body. Finally, the contact pressures between the common sites
88 of pressure ulcers and the sensor are obtained by means of the pressure distribution
89 test sensor. Comparing the calculation results, simulation results and experimental
90 results, the variation in pressure of the body in the supine position is obtained.

91 **Methods**

92 From an anatomical perspective, the pressure ulcers are prone to occur in skeletal
93 protuberance in which the place under pressure and lack of fat protection, no muscle
94 wrap or muscle thin. Without the muscle between the bone and the skin to bear the
95 buffer and decompression, the stress concentration phenomenon will occur in the skin
96 of skeletal protuberance when the skeletal protuberance bears the vertical pressure.
97 The following image shows the typical sites of pressure ulcers in different positions of

98 the human body in the bed (Fig. 1), where the position of pressure ulcers on only one
99 side is shown. The red circles represent the location of pressure ulcers and the area of
100 pressure ulcers that may occur. Because most of the body weight concentrates in the
101 upper body and the stress on one side of the body increases in turning over from the
102 supine position, the typical and main sites of pressure ulcers is focused on the scapula
103 and hip-sacrum in this movement.

104 **Theoretical force analysis of the main pressure ulcer sites**

105 The skeletal protuberance of the shoulder and hip are the main site of pressure
106 ulcers in the process of turning over from the supine position. Furthermore, the
107 vertical force related to shear force is the main factor in the occurrence of pressure
108 ulcers. Therefore, the study on the contact pressure between the skeletal
109 protuberance of the shoulder and hip and the horizontal bed surface can better
110 explain the cause and prevention of pressure ulcers in a different angle of the supine
111 position.

112 The MIMICS (Materialise's interactive medical image control system) software is
113 used to carry out three-dimensional reconstruction of the human skeleton, and the
114 models of the scapula and hip-sacrum were obtained [21,22]. Then, through
115 theoretical analysis and calculation of bone extrusion soft tissue in the process of
116 turning over from the supine position, the contact pressure changes between the
117 main sites of pressure ulcers and the horizontal bed surface will hopefully be
118 obtained. Because the right direction of turning over from the supine position is
119 symmetric with the left direction, the rightward roll motion was analyzed only.

120 The extrusion force on one side of the body increases in turning over from the
121 supine position. Theoretical stress analysis of the scapula in the process of turning
122 over from supine position is shown in Fig. 2. When the angle of the lateral position

123 is θ , the uniformly distributed load is

$$124 \quad F_{N1}=G_{Rsb}+(G_B+G_{Lsb})(1-\cos\theta) \quad (1)$$

125 Where the scapular and the spine initial stress are G_{Rsb} and G_B . The angle between
126 the scapular plane and the chest plane is 30° [23]. Among them, the stress at scapula
127 is respectively F_{N1} and F_{N2} . The gravity around the spine is G_B .

128 In addition to the scapula, the hip-sacrum is also prone to pressure ulcers in turning
129 over from the supine position. The sacrum and tailbone protrude outward from the
130 hip-sacrum in the supine position of the body. Thus, the sacrum and tailbone bear the
131 main body pressure. If the vertical stress of the sacrum and tailbone can be changed to
132 the lateral stress, the incidence of the pressure ulcers will be reduced greatly. The
133 theoretical force analysis of the hip-sacrum in the process of turning over from supine
134 position is shown in Fig. 3. Uniformly distributed load is

$$135 \quad F_{N4}=\lambda G_H+(1-\lambda)(1-\cos\theta)G_H \quad (2)$$

136 Where the gravity at hip-sacrum is G_H . λ is the ratio of the initial weight of one hip
137 to the total weight of the hip G_H . Among them, the stress at sacrum is F_{N3} . The stress
138 at hip is F_{N4} . Based on medical software measurement, the angle between the hip
139 plane and the chest plane is about 45° .

140 When the sacrum does not touch the bed, $F_{N3}=0$.

141 **Biomechanical modeling of the main pressure ulcer sites**

142 Based on the CT scan slices of a healthy man, the three-dimensional reconstruction
143 of the bone was carried out [24]. Then, the three-dimensional bone was imported to
144 the Geomagic Studio software for optimization. Finally, the optimized bone was
145 imported to the ABAQUS for biomechanical modeling [15, 24].

146 The bone is divided into the cortical bone, cancellous bone, articular cartilage and
147 so on, and the material properties of the different parts of the bone are not the same.

148 At present, most studies have simplified the bone into the cortical bone and cancellous
149 bone, and regarded them as homogeneous and isotropic linear elastomers [25]. To
150 simplify the study, the cortical bone and cancellous bone are regarded as the same
151 material properties [26-28]. The Elasticity of the scapula is 9 GPa, Poisson's ratio is
152 0.3 [29]. The Elasticity of the Pelvis is 43.53 GPa and the Poisson's ratio is 0.2 [30].
153 Stress is generated when bones crush soft tissue and stress concentrations lead to
154 pressure ulcers. Although soft tissue includes muscle, skin and so on, in order to
155 improve the efficiency of the simulation, the soft tissue is viewed as a whole and its
156 Elasticity is 200 kPa and the Poisson's ratio is 0.459 [31].

157 Different boundary conditions will be applied to the scapula and hip-sacrum in
158 different states based on the theoretical force analysis of Fig. 2 and Fig. 3. The
159 boundary conditions of five angles of 0° , 30° , 45° , 60° and 90° were set.

160 The details of the model of the scapula and hip-sacrum are used to illustrate the
161 principal constraint setting better, as shown in Fig. 4. In this figure, φ is the angle
162 between the force line and the plane of the shoulder blade, F is the vector force
163 applied to the bone, and represents the direction of the force from the inside out. The
164 force on the left side is always straight down and the angle between the scapula and
165 the horizontal plane changes. The force on the right side always points the horizontal
166 plane from the inside of the hip. Based on the above analysis, principal constraint
167 settings are showed that includes boundary conditions and loads, as shown in Table. 1.
168 For the model details in the Fig. 4, constraints are set to try to keep up with reality.

169
170
171
172
173
174
175

176 **Table 1.** Principal constraint settings between the soft tissue and bone

Angle	Constraint	Scapula	Hip-sacrum
0°	Boundary Conditions	Tie with soft tissue, ③④	Tie with soft tissue, ⑧⑪
	Load	$\varphi=60^\circ$, ⑤	$F=F\cos45^\circ$, ⑫
30°	Boundary Conditions	Tie with soft tissue, ③④⑦	Tie with soft tissue, ⑧⑨⑪
	Load	$\varphi=90^\circ$, ⑤	$F=F\cos75^\circ$, ⑫
45°	Boundary Conditions	Tie with soft tissue, ②③④⑦	Tie with soft tissue, ⑧⑨⑩⑪
	Load	$\varphi=105^\circ$, ⑤	$F=F\cos90^\circ$, ⑫
60°	Boundary Conditions	Tie with soft tissue, ②③④⑦①	Tie with soft tissue, ⑧⑩⑪⑬
	Load	$\varphi=120^\circ$, ⑤	$F=F\cos105^\circ$, ⑫
90°	Boundary Conditions	Tie with soft tissue, ②③④⑦①	Tie with soft tissue, ⑧⑪⑬
	Load	$\varphi=150^\circ$, ⑤	$F=F\cos135^\circ$, ⑫

177

178 **Contact pressure measurement experiment in the process of turning over**

179 In order to explain the laws of motion, and to verify the correctness of the
 180 theoretical analysis and biomechanical modeling, the contact pressure between the
 181 shoulder blade and hip and the bed surface in the process of turning over need to be
 182 measured experimentally. The measurement subject is a healthy volunteer, male, 24
 183 years old, 175cm in height, 70kg in weight, with no adverse health risks, meeting the
 184 requirements of the experiment. Before the experiment, the subject had filled in the
 185 informed consent form and completed the relevant review.

186 The pressure distribution test system is chosen, whose the membrane pressure
 187 sensor manufactured by TEKSCAN of the United States is used. Pressure distribution
 188 test sensor lattice density 0.3 point/cm², range 0.15Kg/cm², high sensitivity, mostly
 189 used for long-term bedridden patients with pressure ulcers monitoring. The sensor
 190 contains a grid of semiconductor substrates, which can change the resistance value of
 191 the internal elements after the load pressure. And the most basic sensor is constituted
 192 by these interlaced matrixes. The resistance data of each sensing element can be
 193 measured through rapid electronic scanning, and the size, time and position of the
 194 force and pressure on the sensor can be obtained through simple calibration function.
 195 The pressure distribution test sensor can complete the real-time acquisition, display

196 and storage of multi-channel sensor information, and can realize the calculation and
197 analysis functions such as the contact image description, the pressure map, contact
198 area and pressure center trajectory of various parts of the human body.

199 Contact pressure measurement experiment in the process of turning over will be
200 performed as shown in Fig. 5. To begin with the subject is lying flat on the pressure
201 sensor, and the shoulder blade is in contact with the sensor. The subject does rollover
202 in an independent supine position, and the pressure change data of the human
203 shoulder blade is collected. Then the subject is lying flat on the pressure sensor, and
204 the hip is in contact with the sensor. The subject does the supine roll with an
205 independent supine position, and the pressure change data of the human hip is
206 collected.

207 **Results**

208 **Theoretical force analysis results**

209 According to the weight parameters of the human body, the following assumptions
210 are made: G_B is 150N, G_{Rsb} and G_{Lsb} are 30N, G_H is 400N. According to human
211 anatomy, the ratio of shoulder blade width at the upper arm to that at the back is about
212 2:3. The ratio λ of the initial weight of one hip to the total weight of the hip G_H is
213 0.5.

214 Considering the contact stress and contact area between the scapula and hip-sacrum
215 and the bed surface are varied, the stress should be used as the standard to evaluate
216 the best lateral position. The length information of the contact area between the
217 scapula and hip-sacrum and bed surface was measured by MIMICS. And then, the
218 area of the contact area was calculated by CAD (Computer Aided Design) and the
219 area in different states was estimated according to the shape of the bone. Finally, the

220 pressure changes of the scapula and hip-sacrum were calculated using the pressure
221 equation $P=F/S$.

222 The theoretical contact pressure of the scapula and hip-sacrum was obtained, as
223 shown in Fig. 6. In this figure, the pressure of the scapula fell slightly within the range
224 0° to 20° , rose a small within the range 20° to 64° and then rose significantly within
225 the range 64° to 90° . And the pressure of hip-sacrum fell largely within the range 0° to
226 50° and rose dramatically within the range 50° to 90° . And the lowest pressure value
227 of the scapula and the hip-sacrum occurred in the 20° and 50° respectively. The d1 is
228 about $1.5e4$ Pa and d2 is about $1.56e5$ Pa.

229 **Finite element analysis results**

230 Based on biomechanical modeling of the main pressure ulcer sites, the finite
231 element simulation of the shoulder and hip is executed, and the stress changes were
232 obtained as shown in Fig. 7.

233 In the stress diagram of the scapula and nearby soft tissue, the upper and lower
234 angles of the scapula, the medial margin, and part of the scapulae are in contact with
235 the nearby soft tissue. And the stress region are mainly occurred in the Area I. Then
236 with the angle of the body in lateral position increased, most of the region of the
237 scapular ridge touches the nearby soft tissue, and the stress changes area gradually
238 concentrates on the Area II. The area of stress concentration achieves a shift from
239 Area I to Area II during the stress change. At a lateral rotation angle of about 30°
240 degrees, the contact area between the scapula and nearby soft tissues is relatively
241 large, and the stress is more evenly distributed over the soft tissues. Lastly, when the
242 lateral position is 90° , stress changes are mainly concentrated on the Area II.

243 In the stress diagram of the hip-sacrum and nearby soft tissue, the tailbone and
244 sacrum are in contact with the nearby soft tissue in the supine position of 0° . And with

245 the angle of the body in lateral position increased, the main stress gradually shifted
246 from Area III to the Area IV and the contact area between the iliac crest and the bed
247 surface is the largest in the lateral position about 45°. The stress difference of the
248 scapula nearby soft tissue d1 is about 6.8e3 Pa between the 0° and 30° and the stress
249 difference of the hip-sacrum nearby soft tissue d2 is about 5.98e4 Pa between the 0°
250 and 45°.

251 The figure (c) shows that the stress of the scapula decreased slightly within the
252 range 0° to 30° and then rose significantly within the range 30° to 90°. Moreover, the
253 stress of the hip-sacrum decreased in the 0° to 45° and increased in the 45° to 90°.
254 And the lowest pressure value of the scapula and the hip-sacrum occurred about the
255 30° and 45° respectively.

256 **Experiment results**

257 The pressure distribution of the shoulder blade and hip was obtained after the
258 experiment, as shown in Fig. 8. The horizontal and vertical lines are used to
259 establish absolute coordinates and the position of the shoulder blades can be got.
260 The geometric center of the shoulder blades is gradually moving to the left sides and
261 the maximum pressure area is gradually moving up to the left. And the geometric
262 center of the hip is gradually moving down to the left sides and the same as the
263 maximum pressure area.

264 In the figure (a), the region (1) and (2) is the pressure region on both sides of the
265 scapula, and the pressure at the scapula is the largest in the supine position. The
266 region (3) in figure (b) is the largest pressure point, and at this moment, the left side
267 of the body gradually disengages from the pressure sensor, and the center of gravity
268 shifts to the right side of the body. Figure(c) shows that the contact area between the
269 human body and the sensor is further shifted to the right side of the body. The largest

270 pressure point in the figure (d) is the region (6) and the mean pressure in the lumbar
271 goes down. This is consistent with the results of the previous theoretical calculation,
272 and verifies the correctness of the theoretical analysis.

273 As shown in figure (e), the region (7) is the sacrum and the largest pressure region
274 is in the sacrum. Figure (f) shows that the maximum pressure region is transferred
275 from the sacrum region to the hip region, and the region (8) moves down to the right
276 of the human body relative to the region (7). The pressure is distributed in most
277 areas of the hip bone, and the contact area is the maximum. Figure (g) shows that the
278 maximum pressure region gradually transferred from the hip region to the greater
279 trochanter, and the region (9) continued to move to the lower right of the human
280 body relative to the region (8), and the pressure distribution gradually concentrated
281 in the region (9). Figure (h) shows that the largest pressure region on concentrate in
282 the region (10), and the contact area decrease. The pressure distribution shows the
283 characteristics of concentration to the dispersion to concentration with the angel
284 increased in turning over from supine position.

285 This figure (i) shows that the stress of the regio scapularis gradually rose within
286 the range 0° to 25° , relatively stable within the range 25° to 40° and rose
287 significantly within the range 40° to 84° . The stress of hip-sacrum gradually fell in
288 the 0° to 40° and increased significantly in the 40° to 90° . And the lowest pressure
289 value of the scapula and the hip-sacrum occurred in the 30° and 40° respectively.
290 The largest pressure change curves of the shoulder blade and hip. d_1 is about $8e3$ Pa
291 and d_2 is about $5.9e4$ Pa. This is consistent with the previous finite element analysis
292 results, which verifies the correctness of the biomechanical modeling.

293 Discussion

294 Based on the anatomical configuration of the human body, the pressure ulcers are

295 prone to occur in skeletal protuberance. The scapula and hip-sacrum are the most
296 prominent bones which have a large area of action on human soft tissue, and most of
297 the body weight concentrates in the upper body, so they can be considered the
298 typical and main sites of pressure ulcers in the process of turning over from supine
299 position. In order to estimate the biomechanical changes on the typical sites of
300 pressure ulcers in the process of turning over, firstly, aimed at the biomechanical
301 research of turning over from the supine position, the pressure distribution of the
302 bone around the trunk's main sites of pressure ulcers was analyzed and theoretical
303 contact pressure between the bone and the bed was calculated. Based on
304 Biomechanical model, the maximum stress change of those bones in different
305 constraint conditions was simulated. Finally, the turning over experiment was
306 carried on and the actual contact pressure between the typical sites of pressure ulcers
307 and the bed was obtained. Theoretical calculation and simulation cannot simulate the
308 real situation, and the experiment is also affected by many factors. But integration of
309 theoretical analysis, experimental and simulation results, their trend and the
310 numerical ratio of the calculation, simulation and the experiment are basically the
311 same, and the study demonstrated the pressure changes of the trunk's typical sites of
312 the pressure ulcers in the process of the turning over [32].

313 The finite element analysis results and the experiment results show that the
314 maximum stress of the scapula and the hip-sacrum and the contact pressure of the
315 shoulder-blade and hip are the same trend, and there is an angle threshold in these
316 results that the contact pressure is smallest. An assisted exoskeleton robot designed
317 for this angle threshold can keep the minimum pressure when the body is in contact
318 with the bed. At the same time, the changes of the body's center of gravity are also
319 known by the contact pressure cloud diagram, and it can provide a design principle

320 that how to control the body's center of gravity and the assisted force. Relevant
321 findings could be applied to pressure ulcer care, as well as assisted robotic control
322 that follows the same trajectory as the human body.

323 Since the internal pressure of bone is not considered in the theoretical calculation
324 and the boundary conditions set by finite element simulation are too ideal and too
325 few, the theoretical calculation results and experiment results are certainly limited.
326 In the following study, it will be further studied that the biomechanics of human
327 bones in the process of turning over and to try to simulate the stress of bones in real
328 situations.

329 **Conclusion**

330 In view of the current studies about compression of the typical sites of pressure
331 ulcers are less, but pressure ulcer care is particularly important, so its biomechanics
332 study is conducted, and the biomechanical changes on the typical sites of pressure
333 ulcers in the process of turning over from supine position are revealed based on
334 theoretical analysis, simulation and experiment. Among them, the complex skeletal
335 movement was simplified into a staged mechanical model under the characteristic
336 state to describe the contact between the typical sites of pressure ulcers and the bed
337 surface during the whole rollover process, and the relationship between the contact
338 pressure and angle is obtained. The results of calculation, simulation and experiment
339 show the following rules: with the increase of the angle of turning over, the pressure
340 on the shoulder increased gradually and the pressure on the hip decreased first and
341 then increased. There is a phenomenon that the two lowest values appeared in the
342 process of turning over and the largest value appeared in the position of 90°, and it
343 suggests that turning over can relieve the high contact pressure between the body
344 and the bed surface. At the same time, the largest pressure value occurs in the

345 position of 90° shows that the body position in a large angle of turning over should
346 not be kept for long time. There may be an optimal angle for pressure ulcer care
347 based on the smallest contact pressure of the typical sites. Decompression devices
348 designed based on this threshold (such as the assisted rollover robot) have better
349 decompression effects, and clinical care guided by this threshold can effectively
350 reduce the occurrence and recurrence of pressure ulcers. And the related results were
351 helpful to provide a reference for clinical nursing.

352 **Abbreviations**

353 CT: Computed tomography; MIMICS: Materialise's interactive medical image control
354 system; CAD: Computer Aided Design.

355 **Acknowledgements**

356 The author wishes to thank National Natural Science Foundation of China (Grant
357 No. 52005045), and National Key R&D Program of China (Grant No.
358 2019YFC0119200), and Natural Science Foundation of Beijing Municipality (Grant
359 No. 19L2018) that supported this work.

360 **Funding**

361 This study was funded by National Natural Science Foundation of China (Grant No.
362 52005045), and National Key R&D Program of China (Grant No. 2019YFC0119200),
363 and Natural Science Foundation of Beijing Municipality (Grant No. 19L2018).

364 **Availability of data and materials**

365 Data are available from the corresponding author upon reasonable request.

366 **Ethics approval and consent to participate**

367 The study was performed following the principles outlined in the Helsinki Declaration
368 and it was approved by Clinical Research Ethics Committee. all the participants gave
369 their informed consent.

370 **Conflict of Interests**

371 There are no conflicts of interest in this study.

372 **Consent for publication**

373 Consent for publication of individual data has been obtained from all the participants
374 of the study.

375 **Authors' contributions**

376 All authors have made substantial contribution to this paper. among them, Peng Su
377 and Leiyu Zhang firstly put forward to the conception of the study and QingLong Lun
378 drafted the article then Peng Su revised it critically for intellectual content. And
379 Qinglong Lun, Da Lu, Tian Liu and QiuLong Wu were responsible to conduct
380 experiment and analyze experiment date. Lastly, all authors read and approved the
381 final manuscript.

382 **Author details**

383 ¹ School of Electromechanical Engineering, Beijing Information Science and
384 Technology University, Beijing, P.R. China. ² School of Biological Science and
385 Medical Engineering, Beihang University, Beijing 100191, P.R. China. ³ Beijing Key
386 Laboratory of Advanced Manufacturing Technology, Beijing University of
387 Technology, Beijing 100124, China

388 **Reference**

389 [1] Jka B, Jc C, Kc D, Kb E, Dan B, H SL. Prevention and treatment of pressure

- 390 ulcers/injuries: The protocol for the second update of the international Clinical
391 Practice Guideline 2019. *J Tissue Viability*. 2019;28(2):51-58.
- 392 [2] Bhattacharya S, Mishra RK. Pressure ulcers: Current understanding and newer
393 modalities of treatment. *Indian J Surg*. 2015;48(1): 4-16.
- 394 [3] Edsberg LE, Black JM, Goldberg M, Mcnichol L, Moore L, Sieggreen M.
395 Revised National Pressure Ulcer Advisory Panel Pressure Injury Staging System.
396 *Journal of WOCN*. 2016;43(6):585-597.
- 397 [4] Yusuf S, Okuwa M, Shigeta Y. Microclimate and development of pressure ulcers
398 and superficial skin changes. *Int Wound J*. 2015;12(1):40-46.
- 399 [5] Zhong W, Malcolm MQ, Q Xing, Pan N, Textiles and Human Skin, Microclimate,
400 Cutaneous Reactions: An Overview. *J Toxicol-Cutan Ocul*. 2006;25(1):23-39.
- 401 [6] Dan L B, Worsley P R. Technologies to monitor the health of loaded skin tissues.
402 *BioMedical Engineering OnLine*. 2018;17(1):40.
- 403 [7] Brem H, Maggi J, Nierman D. High cost of stage IV pressure ulcers. *Am J Surg*.
404 2010;200(4):0-477.
- 405 [8] Mc Ginnis, Briggs M, Collinson M. Pressure ulcer related pain in community
406 populations: a prevalence survey. *BMC Nurs*. 2014;13(1):16.
- 407 [9] Kumari S, Sharma D, Rana A, Pathak R, Lal R, Kumar A. Risk assessment tool
408 for pressure ulcer development in Indian surgical wards. *Indian J Surg*.
409 2015;77(3):206-212.
- 410 [10] Romanelli M, Clark M, Gefen A, *Science and Practice of Pressure Ulcer*
411 Management. London: Springer; 2018.
- 412 [11] Wound, Ostomy and Continence Nurses Society-Wound Guidelines Task Force.
413 WOCN 2016 Guideline for Prevention and Management of Pressure Injuries
414 (Ulcers). *Journal of WOCN Official Publication of the Wound Ostomy &*

- 415 Continence Nurses Society. 2017;44(3).
- 416 [12] Pickham D, Ballew B, Ebong K, Shinn J, Lough ME, Mayer B. Evaluating
417 optimal patient-turning procedures for reducing hospital-acquired pressure ulcers
418 (LS-HAPU): study protocol for a randomized controlled trial. *Trials*.
419 2016;17(1):190.
- 420 [13] Ning L, Peng Y, Yang T, Liang Z, Liu L, Bio-inspired wearable soft upper-limb
421 exoskeleton robot for stroke survivors. 2017 IEEE International Conference on
422 Robotics and Biomimetics (ROBIO). IEEE. 2017.
- 423 [14] Seo KH, Choi TY, Oh C. Development of a robotic system for the bed-ridden.
424 *Mechatronics*. 2011;21(1):227-238.
- 425 [15] Mohammad, Karimi, Timon, Rabczuk, Mauludin, Luthfi. An evaluation of the
426 efficiency of endpoint control on the correction of scoliotic curve with brace. A
427 case study. *Acta Bioeng Biomech*. 2019;21(2):3-10.
- 428 [16] Derler S, Rao A, Ballistreri P, Huber R, Scheel-Sailer A, & Rossi R M. Medical
429 textiles with low friction for decubitus prevention. *Tribology International*.
430 2012;46(1):208-214.
- 431 [17] Rotaru GM, Pille D, Lehmeier FK. Friction between human skin and medical
432 textiles for decubitus prevention. *Tribology International*. 2013;65:91-96.
- 433 [18] V Luís, R Amílcar, Friction of Human Skin against Different Fabrics for Medical
434 Use. *Lubricants*. 2016;4(1):6.
- 435 [19] Defloor T. The effect of position and mattress on interface pressure. *Applied*
436 *Nursing Research Anr*. 2000;13(1):2-11.
- 437 [20] Oomens CWJ, Broek M, Hemmes B. How does lateral tilting affect the internal
438 strains in the sacral region of bed ridden patients? - A contribution to pressure
439 ulcer prevention. *Clin Biomech*. 2016;35:7-13.

- 440 [21] Sulagna, Sarkar, Tikeshwar, Prasad, Sahu, Arijit, Datta, Nimesh, Chandra.
441 Arindam Mechanical response at peri-implant mandibular bone for variation of
442 pore characteristics of implants: A Finite Element Study. *Acta Bioeng Biomech.*
443 2019;21(2):83-93.
- 444 [22] Kruszewski A, Piszczatowski S, Piekarczyk P, Kwiatkowski K. Evaluation of
445 stabilization of intra-articular fracture of distal humerus - finite element study.
446 *Acta Bioeng Biomech.* 2020;22(1):153-163.
- 447 [23] Ingram D. *Musculoskeletal Model of the Human Shoulder for Joint Force*
448 *Estimation.* Epfl. 2015.
- 449 [24] Shu J, Wang Q, H Ma, H Teng, Liu Z. Biomechanical study on the changes of
450 stress in temporomandibular joints after the orthognathic surgery in patients with
451 mandibular prognathism: a 3D finite element study. *Acta Bioeng. Biomech.*
452 2020;22(2):155-163.
- 453 [25] Shih-Chieh, Yang, Pao-Hsin, Liu, Yuan-Kun. Investigation of pullout strength in
454 different designs of pedicle screws for osteoporotic bone quality using finite
455 element analysis. *Acta Bioeng Biomech.* 2019;21(3):57-66.
- 456 [26] Schnackenburg K E, Macdonald H M, Ferber R, Wiley J P, Boyd S K. Bone
457 quality and muscle strength in female athletes with lower limb stress fractures.
458 *Med Sci Sprots Exerc.* 2011;43(11):2110-2119.
- 459 [27] Boyle C, Kim IY. Comparison of different hip prosthesis shapes considering
460 micro-level bone remodeling and stress-shielding criteria using
461 three-dimensional design space topology optimization. *J Biomech.*
462 2011;44(9):1722-1728.
- 463 [28] Martelli S, Taddei F, Cristofolini L. Extensive risk analysis of mechanical failure
464 for an epiphyseal hip prosthesis: a combined numerical-experimental approach.

- 465 Proc Inst Mech Eng H. 2011;225(2):126-140.
- 466 [29] Ahir SP, Walker PS, Squire-Taylor CJ, Blunn GW, Bayley J. Analysis of glenoid
467 fixation for a reversed anatomy fixed-fulcrum shoulder replacement. J Biomech.
468 2004;37(11): 1699-1708.
- 469 [30] Polikeit A, Nolte LP, Ferguson SJ. The effect of cement augmentation on the load
470 transfer in an osteoporotic functional spinal unit: finite-element analysis. Spine
471 (Phila Pa 1976). 2003;28(10):991-996.
- 472 [31] Zhang L, Zhu M, Shen L, Liu Z. Finite element analysis of the contact interface
473 between trans-femoral stump and prosthetic socket. Conference of the IEEE
474 Engineering in Medicine and Biology Society. 2013:1270-1273.
- 475 [32] Nakhli Z, Hatira B, Pithioux M, Chabrand, P, Saanouni K, On prediction of the
476 compressive strength and failure patterns of human vertebrae using a
477 quasi-brittle continuum damage finite element model. Acta Bioeng Biomech.
478 2019;21(2).

479 **Legends**

- 480 Fig.1 The typical sites of pressure ulcers in turning over from supine position.
- 481 Fig.2 Theoretical force analysis of the scapula in the process of turning over from
482 supine position.
- 483 Fig.3 Theoretical force analysis of the hip-sacrum in the process of turning over from
484 supine position.
- 485 Fig.4 Details of the model of the scapula and hip-sacrum.
- 486 Fig.5 The measurement of the contact pressure distribution.
- 487 Fig.6 The theoretical contact pressure of the scapula and hip-sacrum and the bed in
488 different angle.
- 489 Fig.7 The finite element analysis outcome of the soft tissue of scapula and

490 hip-sacrum.

491 Fig.8 The pressure distribution changes of scapula and hip in turning over from supine

492 position.

Figures

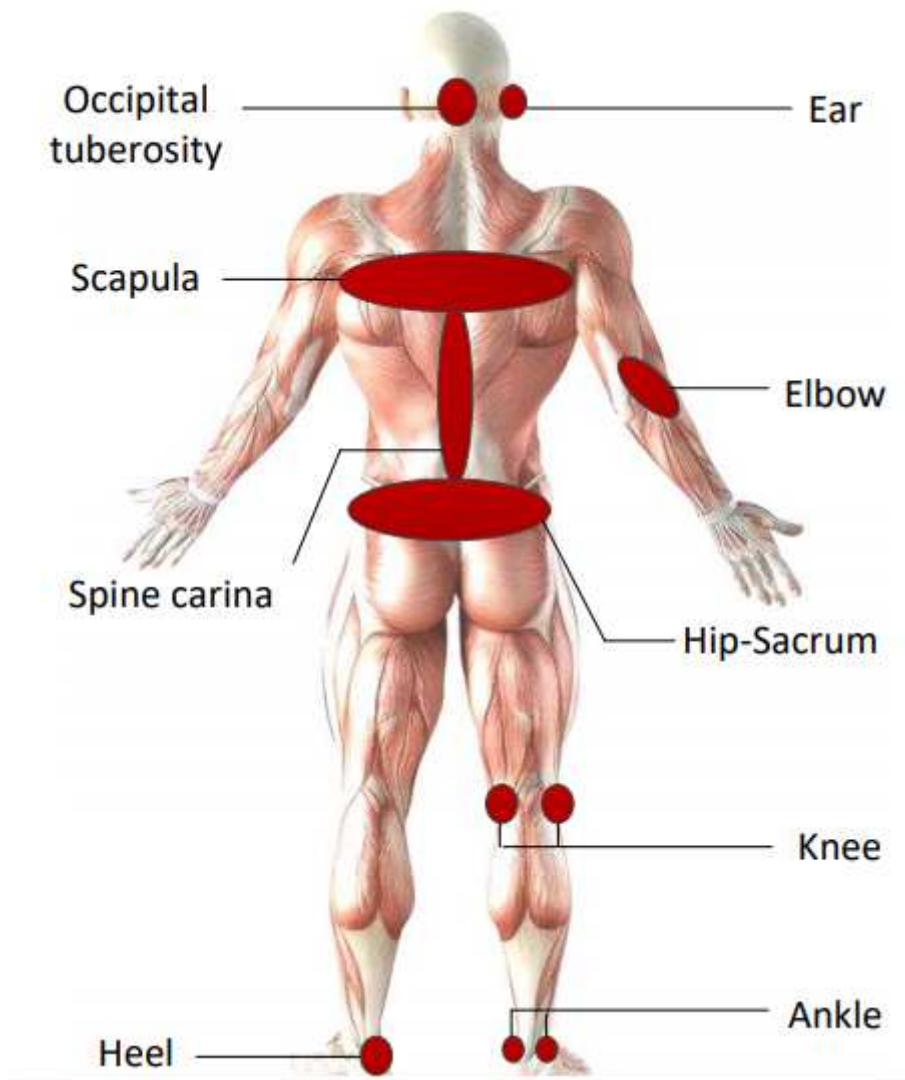


Figure 1

The typical sites of pressure ulcers in turning over from supine position.

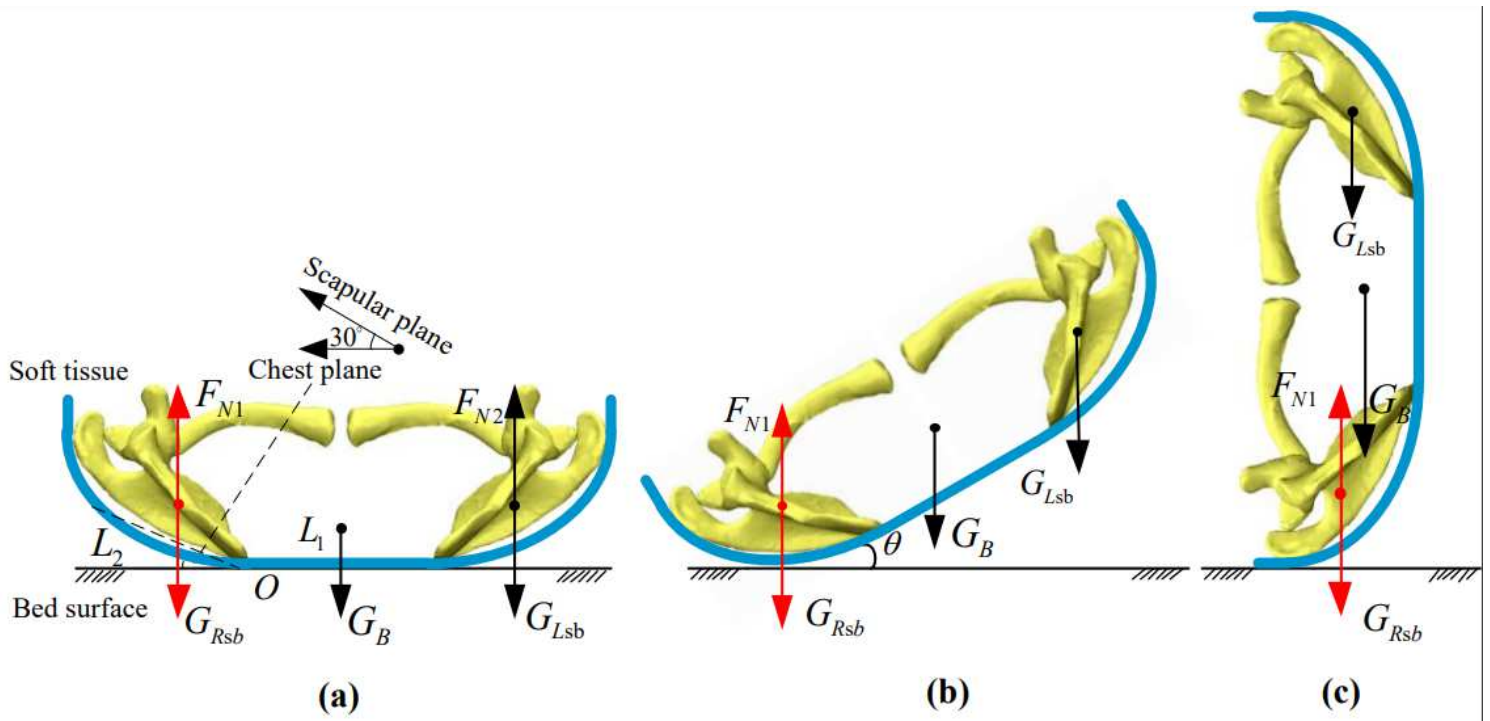


Figure 2

Theoretical force analysis of the scapula in the process of turning over from supine position.

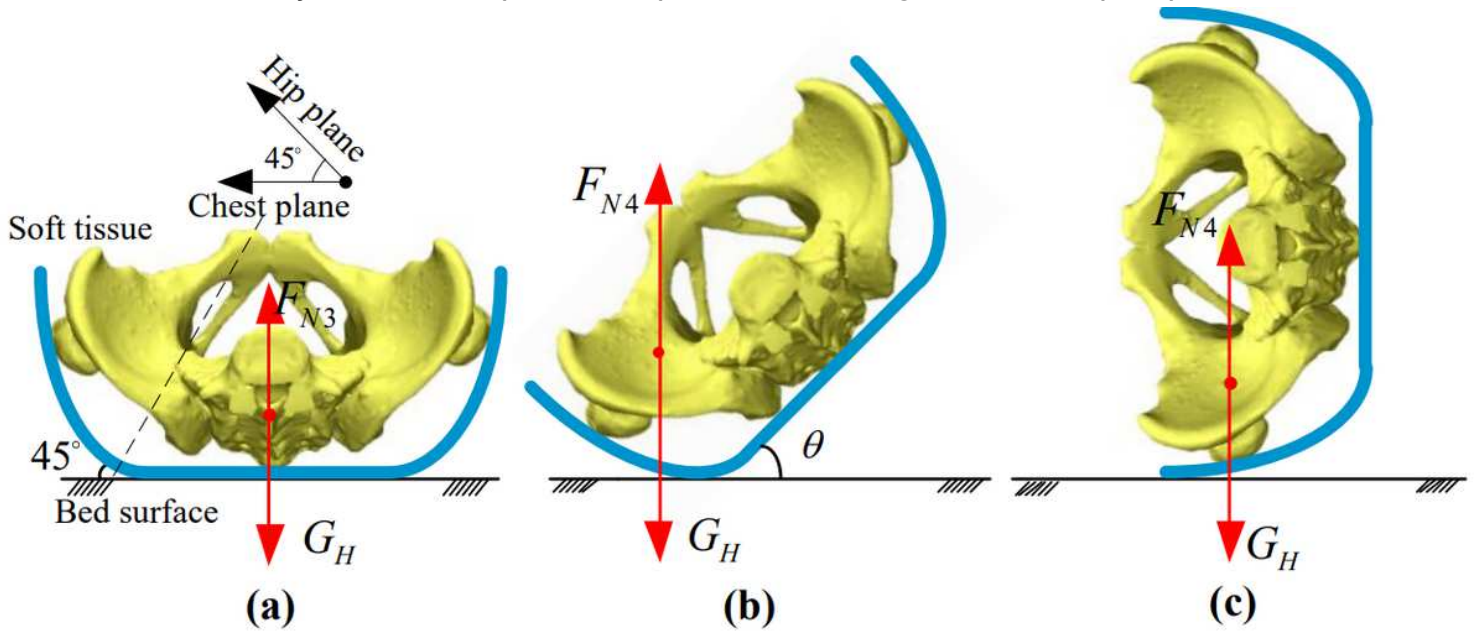


Figure 3

Theoretical force analysis of the hip-sacrum in the process of turning over from supine position.

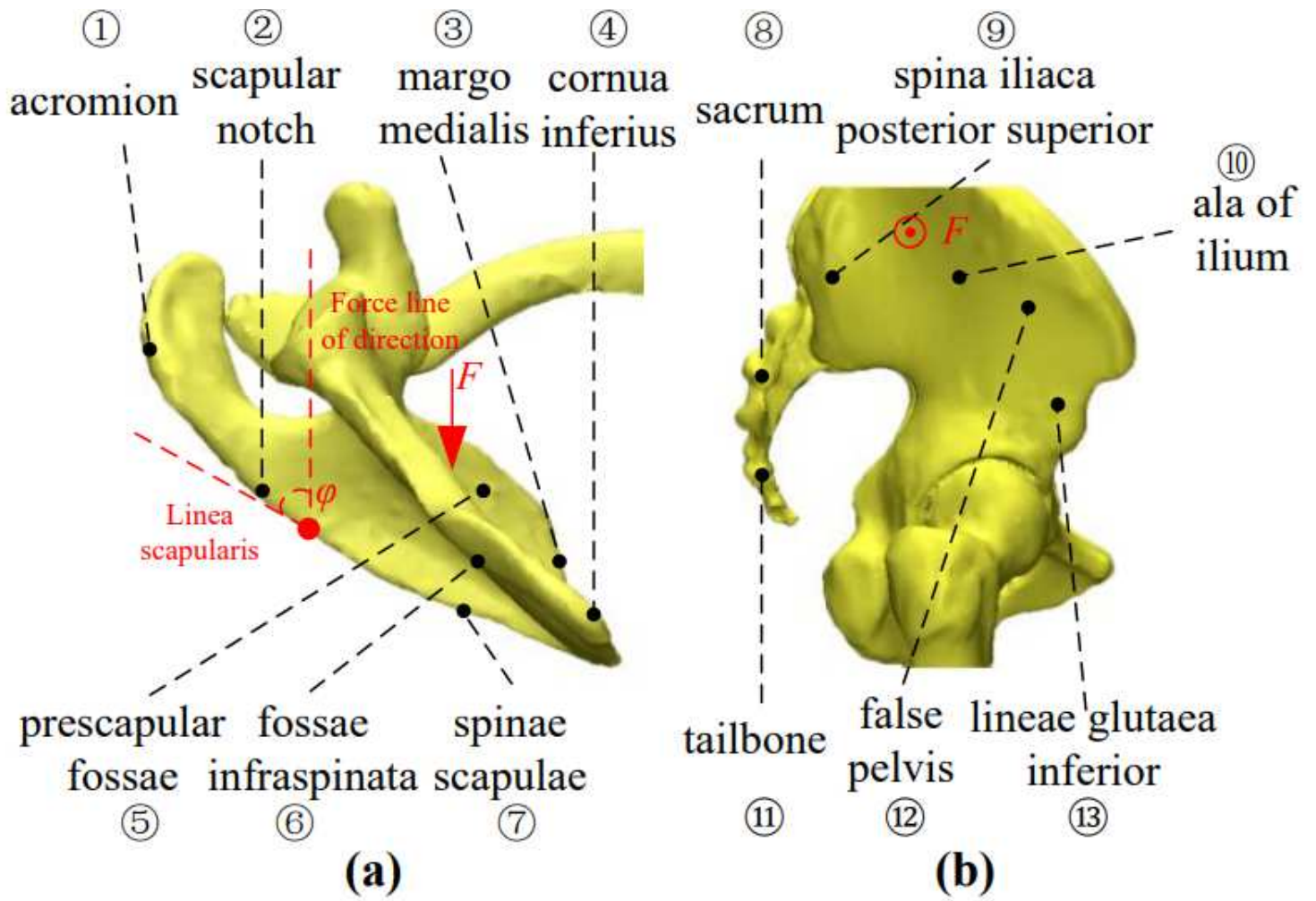


Figure 4

Details of the model of the scapula and hip-sacrum.

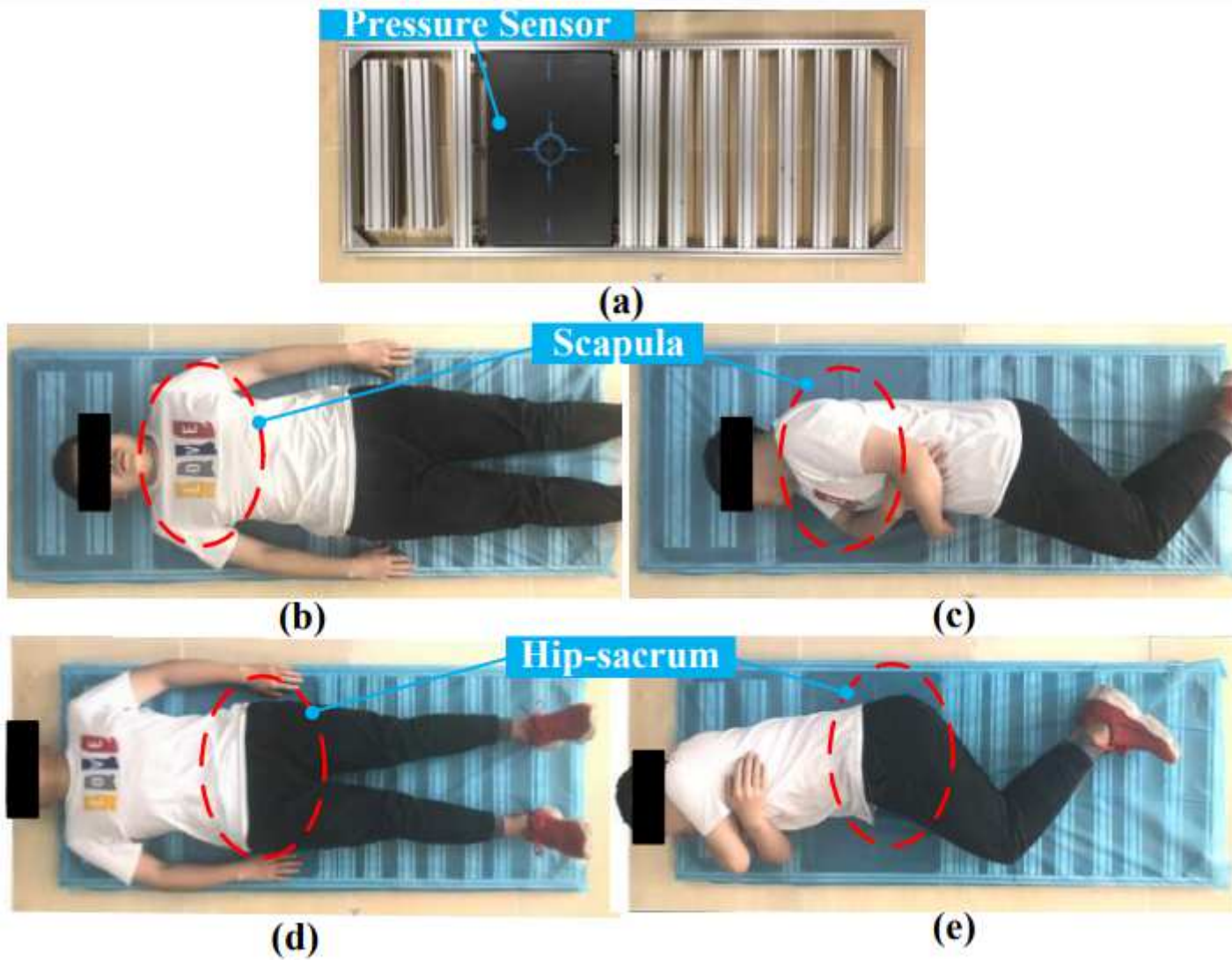


Figure 5

The measurement of the contact pressure distribution.

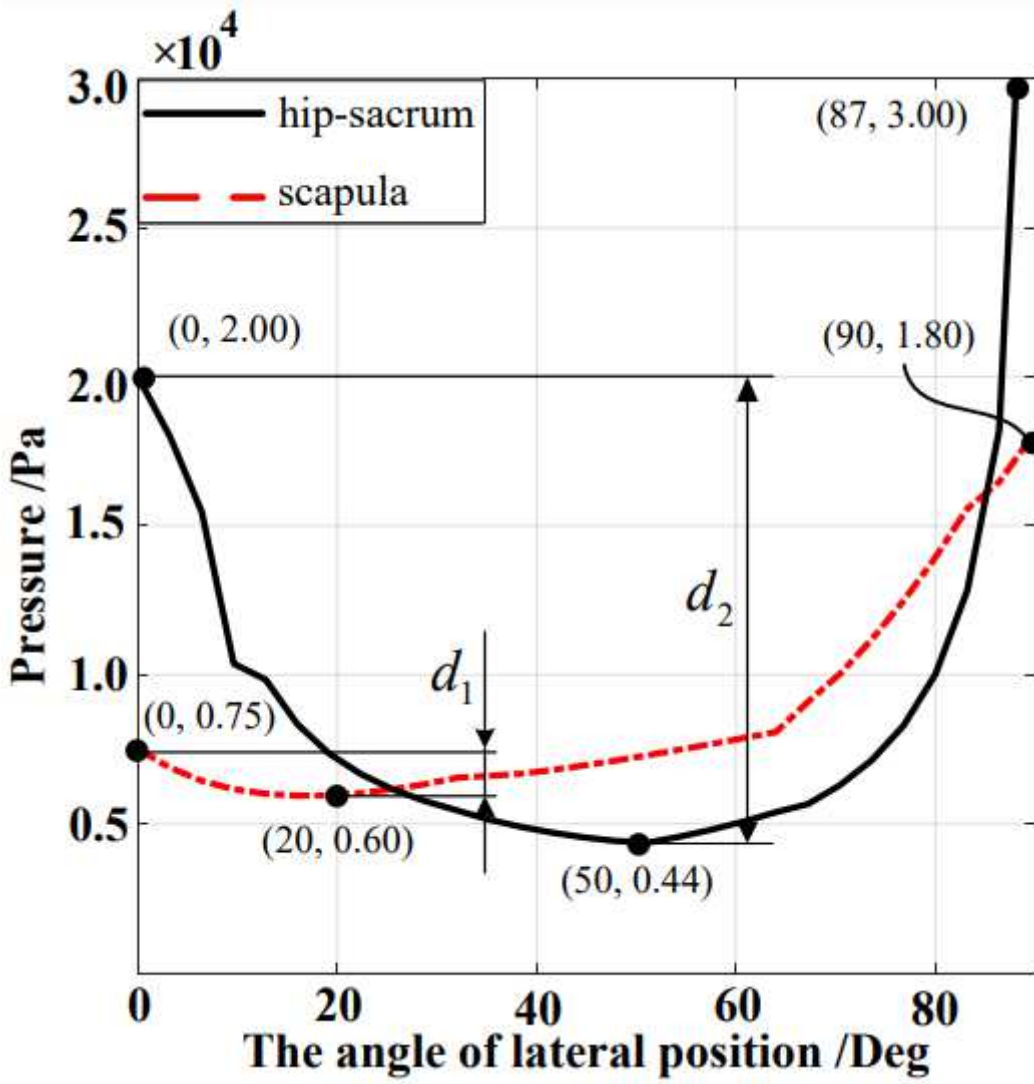


Figure 6

The theoretical contact pressure of the scapula and hip-sacrum and the bed in different angle.

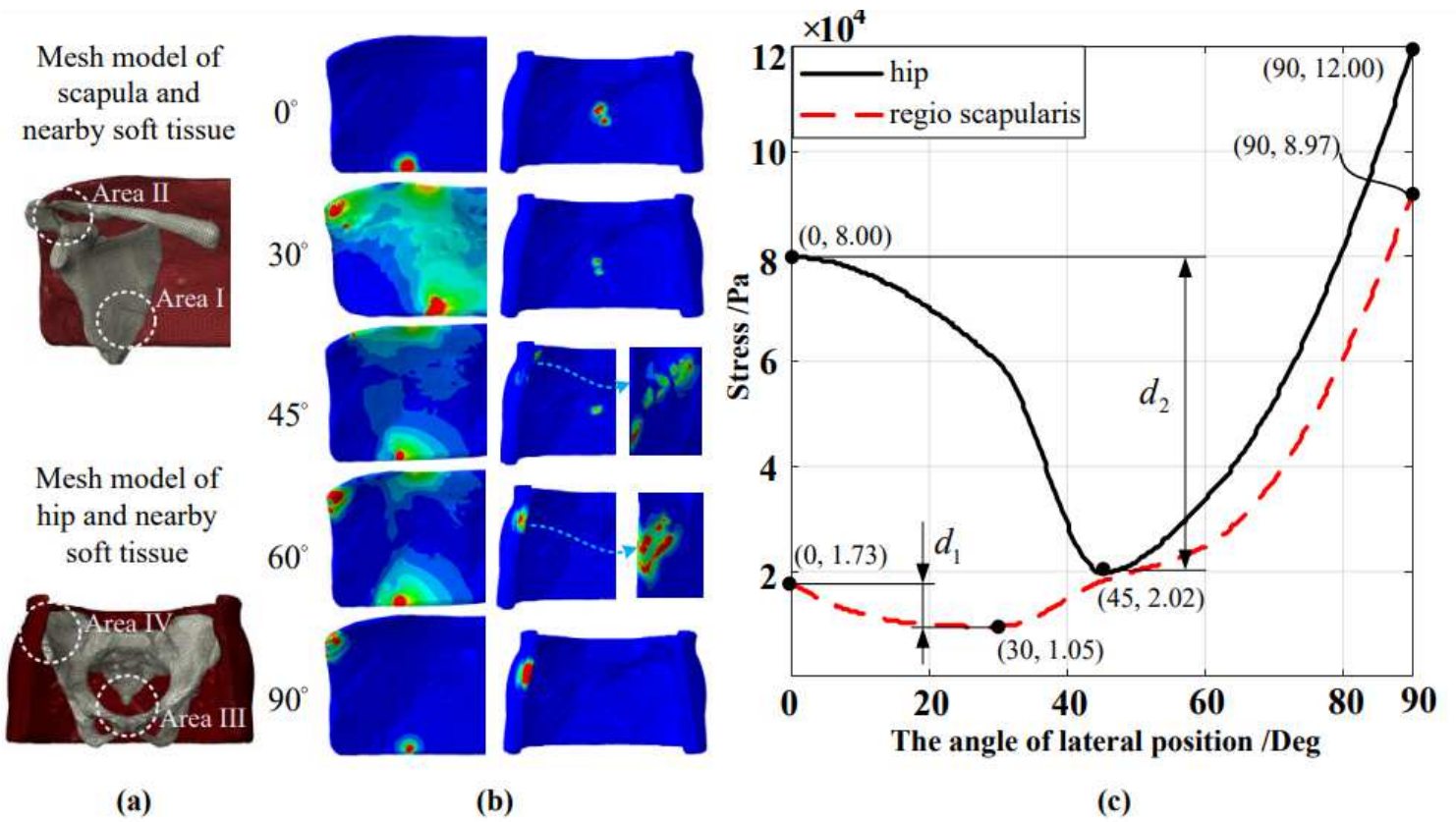


Figure 7

The finite element analysis outcome of the soft tissue of scapula and hip-sacrum.

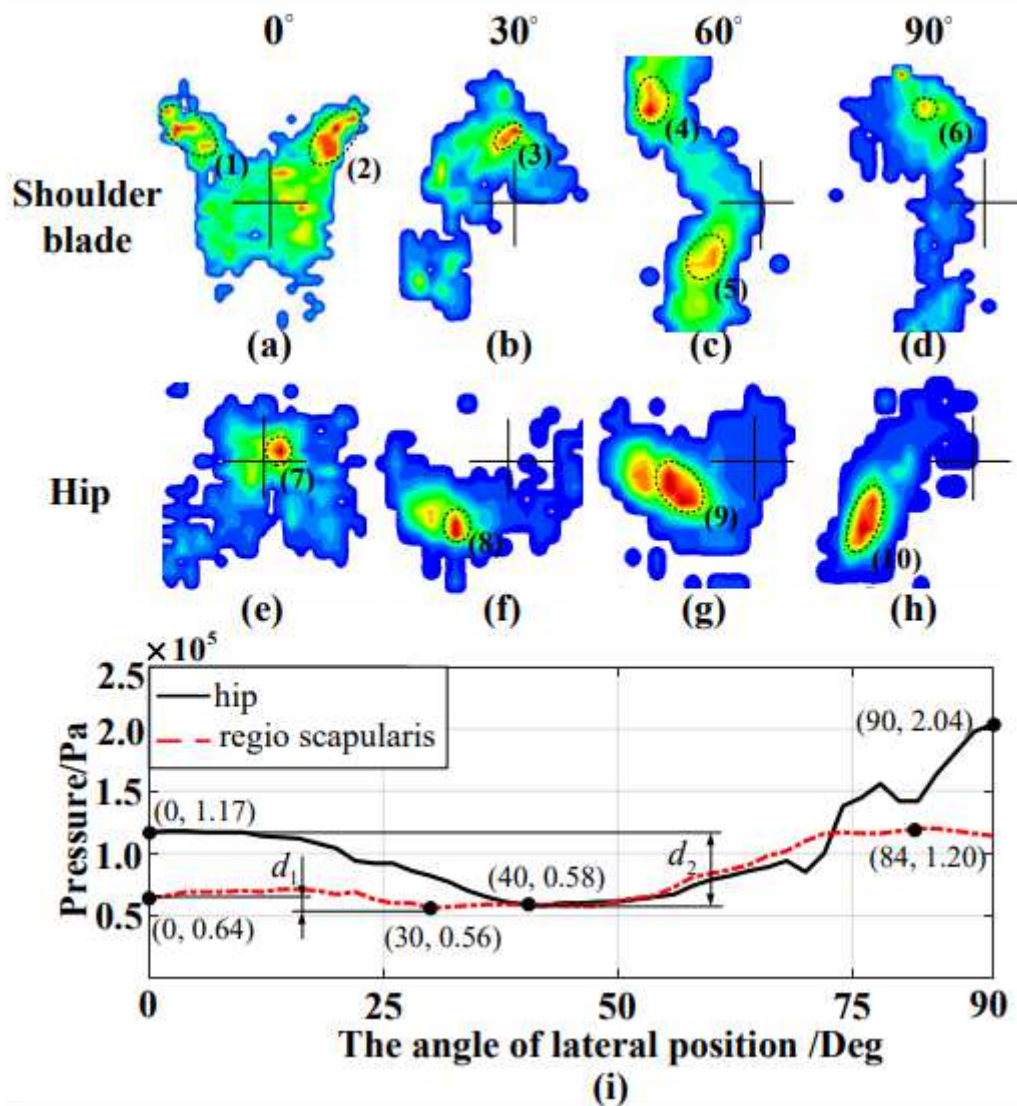


Figure 8

The pressure distribution changes of scapula and hip in turning over from supine position.